Synthesis and Characterization of a Terpolymer Derived from Styrene, Methyl Styrene, and Polyaniline and Its Organoclay Nanocomposite

Mojtaba Abbasian,[1] Mehdi Jaymand,[1] Solmaz Esmaeily Shoja Bonab[2]

[1]*Laboratory of Chemistry Research, Faculty of Science, Payame Noor University, Tabriz, Iran*
[2]*Laboratory of Materials, Faculty of Engineering, Islamic Azad University, Bonab branch, Bonab, Iran*

Received 4 February 2010; accepted 27 July 2011
DOI 10.1002/app.35391
Published online 28 December 2011 in Wiley Online Library (wileyonlinelibrary.com).

ABSTRACT: A synthetic route for the preparation of a novel solution terpolymer derived from styrene, methyl styrene, and polyaniline (PANI) and its organoclay nanocomposite with conductive and mechanical properties is demonstrated. Soluble PANI was synthesized by the incorporation of brominated poly(styrene-*co*-methyl styrene) onto the emeraldine form of PANI. Styrene-*co*-methyl styrene copolymer was synthesized via nitroxide-mediated living radical polymerization by 2,2,6,6-tetramethylpiperidinyloxy iniferter and then was brominated with *N*-bromosuccinimide. The solution terpolymer derived from styrene, methyl styrene, and PANI was synthesized through the *N*-grafting reaction of deprotonated PANI and brominated terpolymer. Nanocomposites of the terpolymer with modified montmorillonite were prepared with a solution intercalation method. The conductivity of the terpolymer was measured by the four-point probe method. The structures of the intermediate, terpolymer, and nanocomposite were investigated by Fourier transform infrared spectroscopy, ^{1}H-NMR, and X-ray diffraction techniques. The molecular weight of the terpolymer was determined by gel permeation chromatography. Their thermal behavior was examined by differential scanning calorimetry and thermogravimetric analyses. © 2011 Wiley Periodicals, Inc. J Appl Polym Sci 125: E131–E140, 2012

Key words: conducting polymers; graft copolymers; living polymerization; nanocomposites; polymer synthesis and characterization

INTRODUCTION

Polyaniline (PANI) has received extensive attention in recent years because of its good electrical conductivity, stability under ambient conditions, and controllability of its electronic and optical properties through variation of the degree of oxidation and protonation.[1] It has been used in applications such as organic, lightweight batteries,[2] microelectronics,[3] electrorheological fluids,[4] and chemical sensors.[5,6] However, like many other conducting polymers, unsubstituted PANI is intractable and suffers from poor processability, mainly because of its rigid and highly conjugated backbone. Several methods have been adopted to overcome their poor processability.

For example, self-doped PANI with sulfonic acid groups substituted onto the polymer were synthesized.[7] Several ring- and *N*-substituted PANIs, soluble in common organic solvents, were prepared directly from the polymerization of the corresponding aniline monomers.[8] The incorporation of side groups into PANI enhanced its solubility and processability and changed its properties.[9] Hosseini[10] reported the growing of aniline onto functionalized polystyrene (PSt). Another approach toward soluble PANI was the copolymerization of aniline with suitable substituted aniline to produce copolymers. The obtained copolymers had improved in solubility.[11] To improve the melt and solution processability, the majority of PANI modifications to date have been made by the incorporation of substituents on the polymer backbone.[12] Flexible alkyl chains,[13] poly(ethylene glycol) chain,[14] and polyether chain[15] have been incorporated onto PANI through the *N*-alkylation method. Furthermore, when PANI has been compounded with inorganic nanoparticles, the PANI composites have usually exhibited more special properties than pure PANI.[16] For example, PANI/Fe_3O_4 nanocomposites were more promising electromagnetic wave absorbers than pure PANI and pure Fe_3O_4 particles.[17] PANI with the addition of MnO_2 and ZrO_2 nanoparticles could change to be water-dispersible.[18] Also, PANI/TiO_2 nanocomposites[19] had high piezoresistivity, and PANI that was inserted between silicate layers could be easily oxidized and polymerization initiated in an electronic field because the presence of the negatively charged silicate layers stabilized the radical cation and promoted the polymerization.[20–22]

Correspondence to: M. Abbasian (m_abbasian20@yahoo.com or m_abbasian@pnu.ac.ir).

Contract grant sponsors: Iran National Science Foundation, Tabriz Payame Noor University.

In this article, a new *N*-substituted PANI was synthesized by the insertion of a bromine-dangled (styrene–methyl styrene) copolymer onto the PANI backbone. PSt derivatives are gaining wide recognition, as they possess many unique properties, such as solubility in organic solvents and good mechanical properties. Thus, the incorporation of PSt derivatives into PANI may endow the resulting copolymer with new and interesting properties. For instances, the process may enhance the solubility and processability of PANI. Styrene-*co*-methyl styrene copolymer was synthesized via a nitroxide-mediated living radical polymerization (NMRP) technique by 2,2,6,6-tetramethylpiperidinyloxy (TEMPO). The nitroxide-mediated polymerization method is a controlled free-radical methodology, which allows the synthesis of star and graft copolymers with controlled molecular weights under mild conditions. This polymerization method is based on the use of a traditional radical initiator (e.g., benzoyl peroxide) in the presence of a stable nitroxide radical (e.g., TEMPO).[23–25]

In this work, the terpolymer poly(styrene-*co*-methyl styrene) [poly(St-*co*-MSt)]-grafted-PANI was synthesized by the incorporation of brominated poly(styrene-*co*-methyl styrene) [poly(St-*co*-MSt)-Br] onto the emeraldine form of PANI. The styrene-*co*-methyl styrene copolymer was synthesized via an NMRP technique under an argon atmosphere and then brominated with *N*-bromosuccinimide (NBS) (Darmstadt, Germany) to obtain copolymers with bromine. The solution terpolymer, derived from styrene, methyl styrene, and PANI, was synthesized through the *N*-grafting reaction of deprotonated PANI and brominated terpolymer. Finally, the synthesis of the nanocomposite was carried out by a solution intercalation method in carbon tetrachloride (CCl_4) as a solvent.

EXPERIMENTAL

Materials

Styrene and *p*-methyl styrene (Darmstadt, Germany) were distilled under reduced pressure before use. NBS (Merck) was purified by recrystallization in water at 70°C. 2,2′-Azobis(isobutyronitrile) (AIBN; Aldrich) was recrystallized in ethanol at 50°C before use. TEMPO was prepared by the method reported by our research group previously.[26] Aniline (Merck) was dried with NaOH and fractionally distilled under reduced pressure from NaH or CaH_2. Butyl lithium (BuLi) was purchased from Merck and was titrated with diphenylacetic acid before use. Ammonium persulfate (Merck) was recrystallized at high temperatures from EtOH/water. Hexadecyl trimethyl ammonium chloride salt was purchased from Merck. Sodium montmorillonite (MMT) was obtained from Southern Clay Products (Modsburg, Germany) under the trade name Cloisite NaC. MMT was reported to have an approximate aspect ratio of 250:1 and was a 2:1 tetrahedral/octahedral aluminum silicate smectite mineral with an idealized chemical formula of $Na_{0.33}[Mg_{0.33}Al_{11.67}\ Si_4O_{10}](OH)_2$ and a cation-exchange capacity of 95 mequiv/100 g.

Instrumentation

Fourier transform infrared (FTIR) spectra were recorded with a Shimadzu FTIR-8101M (Tokyo-Japan). The samples were prepared by the grinding of the dry powders with KBr and compression of the mixture to form disks. The disks were stored in a desiccator to prevent moisture absorption. ^{1}H-NMR spectra were recorded on a Fourier transform NMR (400-MHz) Bruker instrument in $CDCl_3$. The conductivity of the polymers was measured by a four-probe apparatus made by Azar Electric, Iran. The molecular weight of the resulting polymer was obtained with a Maxima 820 gel permeation chromatography (GPC) analysis instrument with a PSt (10^6, 10^5, and 10^4 Å) calibration standard with a tetrahydrofuran (THF) mobile phase at a flow rate of 1 mL/min and a column temperature of 30°C. The measurement of the thermal properties of the PSt-*co*-PMSt, (PSt-*co*-PMSt)-*g*-PANI, and (PSt-*co*-PMSt)-*g*-PANI/O—MMT nanocomposites were performed with a thermogravimetric analysis (TGA)–"photoluminescence" spectroscopy instrument (England). Samples of about 10 mg were heated from 25 to 600°C at rate of 10°C/min under a nitrogen flow. Differential scanning calorimetry (DSC) analyses were carried out with a Netzsch instrument (Bavarian, Germany). The sample was first heated to 200°C and kept for 5 min to eliminate the heat history. The sample was then cooled down at a rate of 10°C/min. The sample was then reheated to 200°C at a rate of 10°C/min. The entire test was performed under nitrogen purging at a rate of 50 mL/min. X-ray diffraction (XRD) spectra were obtained with a Siemens D 5000 X-ray generator (Cu Kα radiation with $\lambda = 1.5406$ Å) with a 2θ scan range of 2–80° at room temperature. The dispersion state and layered structure of MMT were observed with a VEGA//TESCAN KX5000 scanning electron microscope (Shanghai, China).

Synthesis of PSt-*co*-PMSt

Styrene (10 mL) and methyl styrene monomers (50/50 v/v) and 0.15 g (0.6 mmol) of benzyl peroxide and 0.14 g (90 mmol/L) of TEMPO were placed in an ampule degassed with several freeze–pump–thaw cycles, sealed off *in vacuo*, and placed in an oil bath at 95°C for 4 h. Then, the temperature was increased to 130°C for another 12 h. Then, the samples were taken from the oil bath and dipped in liquid nitrogen to stop the polymerization. The products were diluted with THF and precipitated in methanol. This

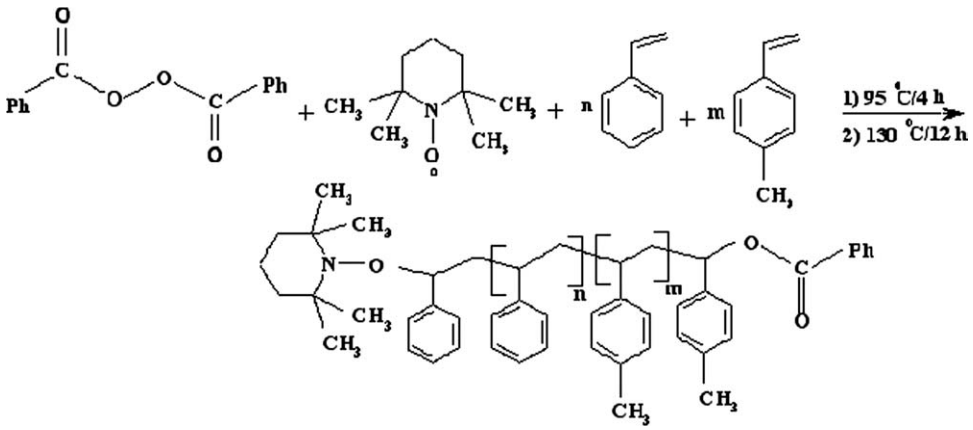

Scheme 1 Synthesis of PSt-*co*-PMSt via NMRP.

product was dried overnight *in vacuo* at room temperature (Scheme 1).

Synthesis of (PSt-*co*-PMSt)-Br

A 100-mL, three-necked flask containing 30 mL of CCl_4 and 0.3 g of poly(St-*co*-MSt) was equipped with a mechanical stirrer under an argon atmosphere. In a separate container, 34 mmol of NBS and 21 mmol of AIBN were dissolved in 10 mL of dried CCl_4. This mixture was added to the polymer solution after the mixture was allowed to stir for 2 h at 70°C under an argon atmosphere. The mixture was cooled at room temperature, and the brominated copolymer was recovered by filtration in methanol. This product was dried overnight *in vacuo*.

Yield: 0.35 g (white powder). FTIR (KBr, cm^{-1}): 3075 (aromatic protons of toluene), 1608 (—C—C— aromatic protons), 1476 (—CH_3 of methyl styrene). ^{1}H-NMR ($CDCl_3$, ppm): 7.55–7.70 (aromatic protons), 4.15–4.25 ppm (—CH_2Br protons of methyl styrene; Scheme 2).

Synthesis of PANI

PANI was synthesized by the oxidative polymerization of aniline according to the method reported in the literature.[27] Thus, 0.1 mol (9.2 mL) of aniline was dissolved in 100 mL of 1.7 mol/L HCl. The solution was kept at 0°C under an argon atmosphere. A prechilled solution of 0.1 mol (22.82 g) of APS in 100 mL of 1.7 mol/L HCl was added slowly with vigorous stirring. The reaction mixture was agitated continuously for another 5 h. The precipitate was subsequently filtered and washed several times with methanol, and finally, a colorless filtrate was obtained [yield = 8.35 g (92%)]. The collected green–black PANI salts were added to an ammonia solution (1.7 mol/L) and stirred for 3 h. The undoped PANI was filtered and washed several times with water. The resulting powder was dried at 50°C under reduced pressure (Scheme 3).

Preparation of (PSt-*co*-PMSt)-*g*-PANI

The reaction flask was dried and kept under an inert atmosphere throughout the reactions by a constant flow of argon. The emeraldine base form of PANI (0.5 g) was dissolved in 50 mL (THF). The solution was cooled to 0°C, and a predetermined amount of BuLi (1 mol) was added with stirring. The color of the solution changed from dark blue to green–black. In another dried flask, 1.5 g of (PSt-*co*-PMSt)-Br (1.5 g) was dissolved in 20 mL of THF under an argon atmosphere. This solution was added to the reaction mixture. The reaction was stirred under an argon atmosphere at 60°C for 24 h. The color of the solution turned blue gradually. The reaction mixture was poured into methanol to precipitate the terpolymer. The precipitate was filtered, added to toluene, and stirred at 30°C for remove the residual amount of unreacted PANI. The polymer solution was filtered

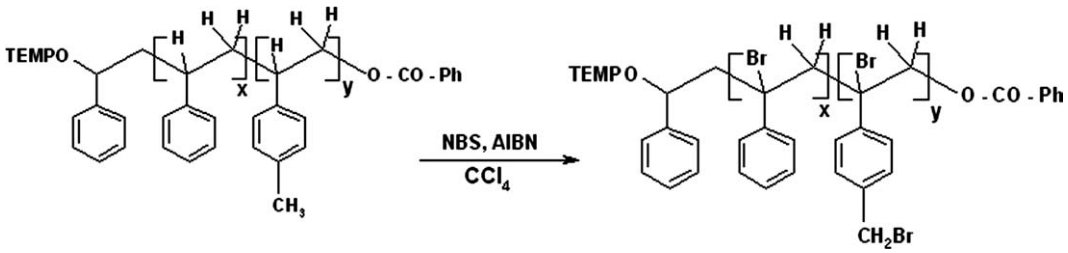

Scheme 2 Synthesis of (PSt-*co*-PMSt)-Br.

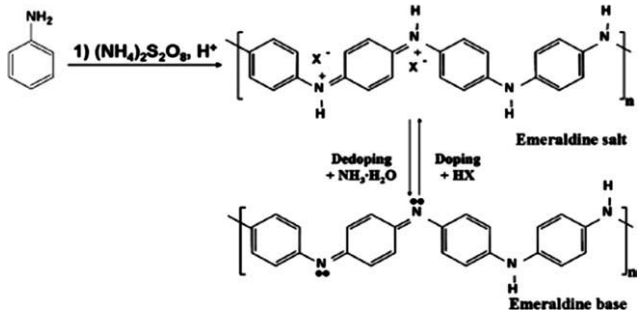

Scheme 3 Synthesis of PANI.

in methanol. This product was dried overnight *in vacuo*. The copolymer was partially soluble in hot cyclohexane, whereas unreacted PSt-*co*-PMSt was completely soluble in hot cyclohexane. In the reaction between (PSt-*co*-PMSt)-Br and polyalanine, when crosslinking reactions took place; the copolymer had to be insoluble in all solvents, whereas the terpolymer could be dissolved in powerful organic solvents, such as dimethylformamide and THF (Scheme 4).

Surface modification of MMT

Organophilic montmorillonite (OMMT) was obtained after treatment with a hexadecyl trimethyl ammonium chloride salt ion-exchange process. MMT was first dispersed in deionized water under ultrasound for 1 h. The modifier was prepared in deionized water separately and was added to the clay dispersion at an amount a little higher than the cation-exchange capacity of MMT. The resulting suspension was intensively stirred for 10 h and then filtered with deionized water three times. The final product was dried *in vacuo* at room temperature for 48 h, after which it was ground into powder.

Preparation of the (PSt-*co*-PMSt)-*g*-PANI/OMMT nanocomposites

The organoclay MMT (0.1 g, 3 wt %) was dispersed in 30 mL of carbon tetrachloride for 30 min under ultrasound, after which 2 g of (PSt-*co*-PMSt)-*g*-PANI was dissolved in 50 mL of carbon tetrachloride. Then, the clay suspension was slowly added to the polymeric solution with constant stirring for 6 h, after which the mixture was poured into 300 mL of methanol for rapid precipitation. The precipitate was filtered and dried at 50°C *in vacuo* for 2 days.

RESULTS AND DISCUSSION

Synthesis of PSt-*co*-PMSt by living polymerization

Living polymerization is characterized by a linear increase of the molecular weight with conversion

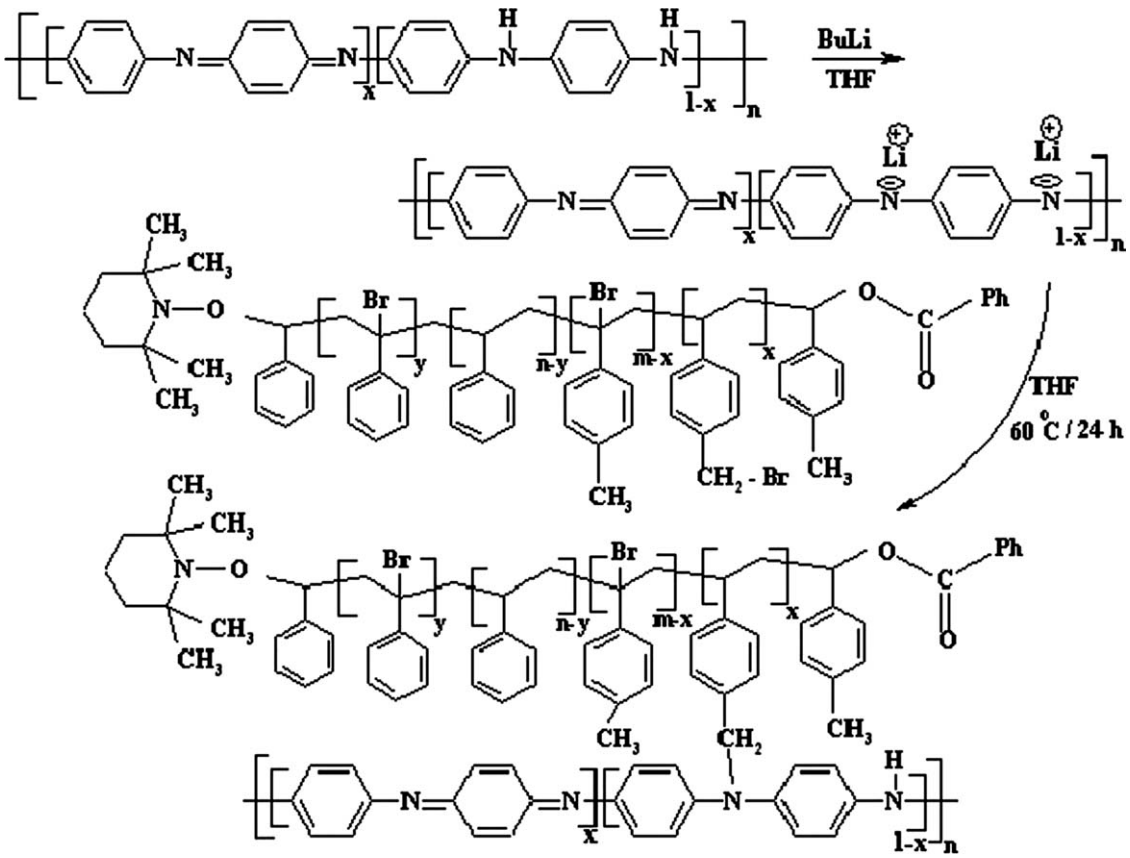

Scheme 4 Preparation of (PSt-*co*-PMSt)-*g*-PANI.

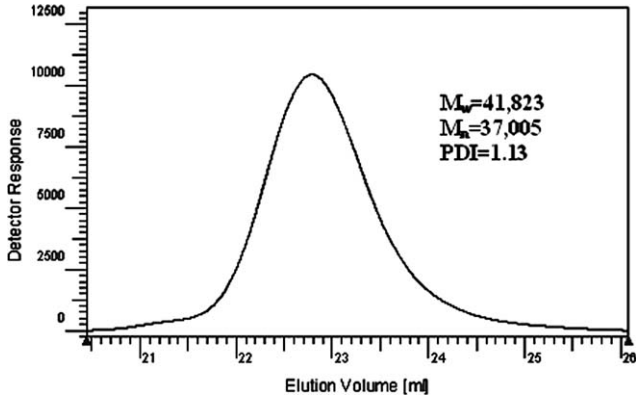

Figure 1 GPC chromatograms of poly(St-*co*-MSt).

and reaction time, and a narrow molecular weight distribution is evidenced by a polydispersity index [PDI = weight-average molecular weight (M_w)/number-average molecular weight (M_n)] approaching 1.[28] Figure 1 represents the GPC chromatograms of the PSt and poly(methyl styrene) (PMSt) copolymer, whose molecular weight distribution by GPC was 1.13. Single GPC curves of the homopolymer clearly indicated that it was the copolymer; if so, the GPC curve should have appeared as two peaks, one for the PSt homopolymer and the other for the PMSt homopolymer.

The monomer conversion was obtained indirectly from the mass of polymer formed. The plot of ln(Molecular weight of the poly (styrene-methyl styrene) in the time of 12 (h), $[M]_0$/Molecular weight of the poly (styrene-methyl styrene) in the time of 15 (h) and 18 (h), [M]) versus time was a straight line passing through the origin; this indicated that the polymerization was first order with respect to monomer concentration, along with a constant number of the growing species; this suggested a controlled NMRP. The results are summarized in Table I.

The GPC trace of the poly(St-*co*-MSt) and poly(St-*co*-MSt)-Br (M_n = 37567, M_w = 45456, PDI = 1.21) was unimodal and showed no tailing or broadening of the molecular-weight distribution; this confirmed that no crosslinking or chain scission occurred during the bromination procedures.

Figure 2 shows the FTIR spectra of the poly(St-*co*-MSt) and brominated copolymer. The FTIR spectra of PSt-*co*-PMSt showed the characteristic absorption bands due to stretching vibration of C—H (3100–2850 cm^{-1}), weak aromatic overtone and combination bands in the 2100–1670-cm^{-1} region, C=C stretching vibrations (1606 and 1485 cm^{-1}), CH_2 bending vibrations (1445 and 1372 cm^{-1}), CH_2—Br bending vibrations (1170 cm^{-1}), and γ(C—H) in the aromatic ring (768 and 709 cm^{-1}). Figure 2(b) exhibits an additional absorption band at 557 cm^{-1}, which was attributed to the C—Br group.

TABLE I
Molecular Weight of the Poly(styrene–methyl styrene) Copolymer at Various Times

Entry	Time (h)	M_n	M_w	M_w/M_n
1	12	37005	41823	1.13
2	15	39863	48235	1.21
3	18	44977	54873	1.22

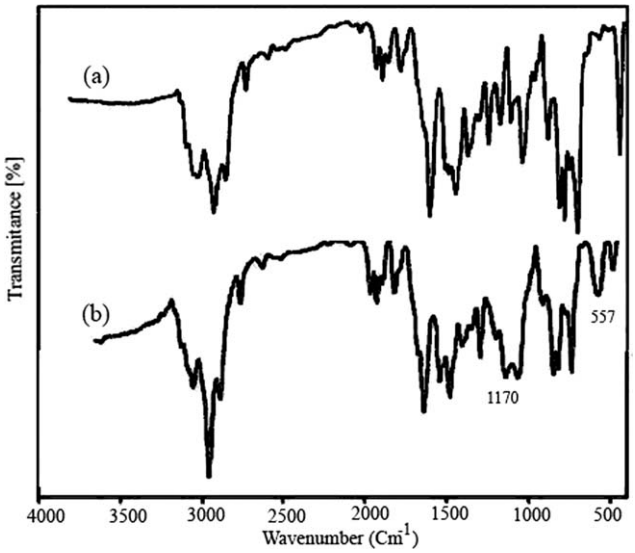

Figure 2 FTIR spectra of (a) PSt-*co*-PMSt and (b) (PSt-*co*-PMSt)-Br.

^{1}H-NMR spectra of the copolymer PSt-*co*-PMSt and brominated copolymer (PSt-*co*-PMSt)-Br are

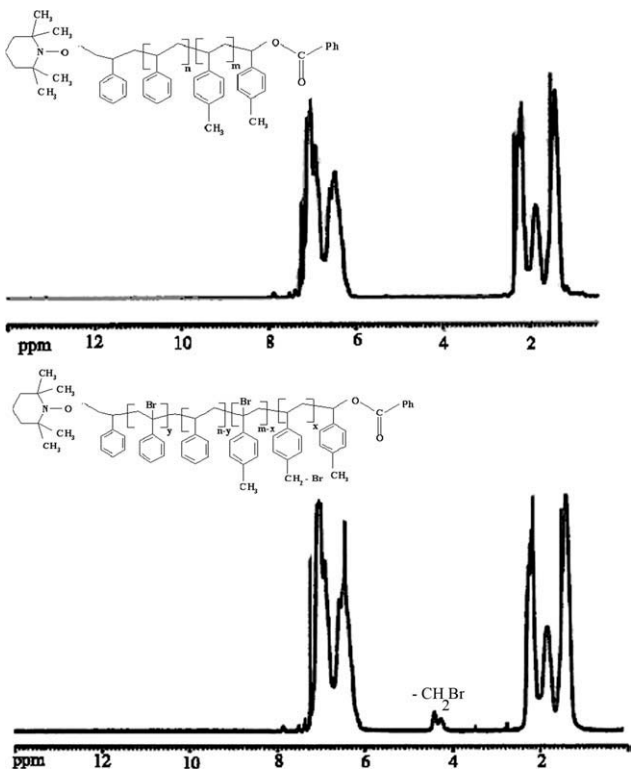

Figure 3 ^{1}H-NMR spectra of (a) PSt-*co*-PMSt and (b) (PSt-*co*-PMSt)-Br.

TABLE II
Compositions of the (PSt-*co*-PMSt)-*g*-PANI Copolymers

Polymer	Composition		
	C%	H%	N%
PANI	76.1	4.6	14.2
(PSt-*co*-PMSt)-*g*-PANI	78.1	6.79	10.01
	Degree of grafting = 2.5%		

shown in Figure 3. The ^{1}H-NMR spectra of the copolymer PSt-*co*-PMSt showed the resonances at about 2.28, 1.86, and 1.43 ppm assigned to the CH_3, CH, and CH_2 units in the copolymer, respectively, and the resonance at about 6.13 to 7.38 ppm was assigned to aromatic protons [Fig. 3(a)]. After bromination, the ^{1}H-NMR spectra showed a resonance at about 4.14–4.57 ppm, which was assigned to the CH_2—Br and CH—Br groups in the brominated copolymer [Fig. 3(b)].

To calculate the extent of bromination for PSt-*co*-PMSt of a particular extent of bromination, the following method was adopted. (PSt-*co*-PMSt)$_m$–[(PSt-*co*-PMSt)-Br]$_n$ represents the brominated PSt–methyl styrene copolymer. The molar percentage of bromination is given by $n/(m + n) \times 100$. The area under the aliphatic region is given by $9m + 6n$, and the area under the aromatic region is given by $9m + 9n$. In Figure 3, the solution of the simultaneous equation with the integrated areas, it can be seen that $9m + 6n = 145.73$ and $9n + 9m = 154.1$, and therefore. $n = 2.79$ and $m = 14.33$. Therefore, the extent of bromination was $2.79/(2.79 + 14.33) \times 100 = 16.29\%$ (Scheme 2).

The elemental analysis was carried out to determine the composition of the copolymers with various elements, such as C, H, and N, present in the polymer matrix. Table II shows the compositions of the poly(St-*co*-MSt)-*g*-PANI. As shown in Table II, the degree of grafting was 2.5%.

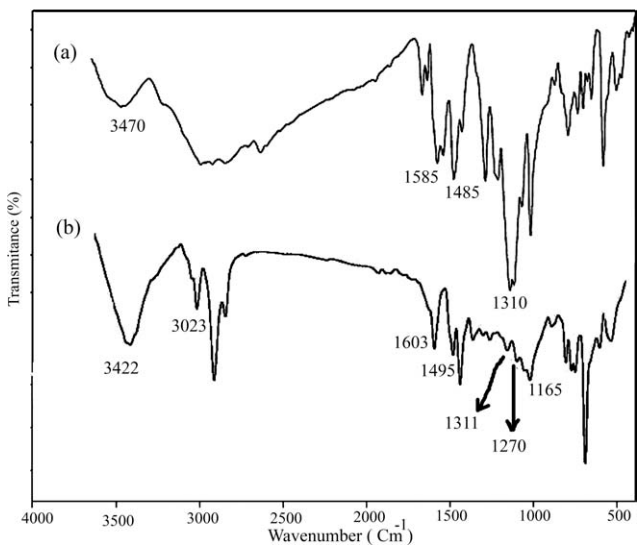

Figure 4 FTIR spectra of (a) PANI and (b) (PSt-*co*-PMSt)-*g*-PAN.

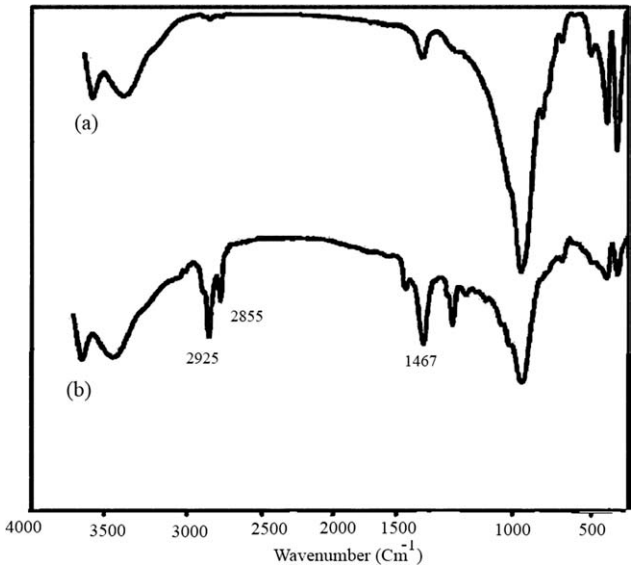

Figure 5 FTIR spectra of the (a) unmodified MMT and (b) modified MMT.

Figure 4(a,b) shows the FTIR spectra of PANI [Fig. 4(a)] and (PSt-*co*-PMSt)-*g*-PANI [Fig. 4(b)]. In this spectra of PANI, the C=N in the quinoidal units appeared at 1585 cm^{-1}, the benzenoid stretching appeared at 1485 cm^{-1}, and the N—H stretching appeared at 3470 cm^{-1}.

After the grafting of PANI onto PSt-*co*-PMSt, the absorption band of PANI, namely, the C=N in the quinoidal units, appeared at 1603 cm^{-1}, the benzenoid stretching appeared at 1497 cm^{-1}, the N—H stretching appeared at 3422 cm^{-1}, and the aromatic C—H stretching appeared at 3023 cm^{-1}. The $C_{aromatic}$—N stretching band of an aromatic amine appeared at 1310 cm^{-1}. The absorption band at 1165 cm^{-1} was characteristic of electron-like absorption of the N=Q=N vibration (where Q denotes the quinoid ring).[29] The presence of the absorption band at 1270 cm^{-1}, attributed to aliphatic C—N stretching, suggested that the PSt and PMSt chains were linked on the nitrogens of PANI, whereas neither the position nor the intensity of the aromatic C—N stretching band at 1311 cm^{-1} changed after grafting.[30] The absorption band at 817 cm^{-1} was characteristic of the out-of-plane bending vibration of the 1,4-disubstituted benzene ring. PSt and PMSt had characteristic bands at 2921 and 2853 cm^{-1}, attributed to aliphatic C—H stretching, and at 759 and 699 cm^{-1}, corresponding to out-of-plane hydrogen deformation, which indicated the existence of the PSt and PMSt chains in our samples.[31]

Conductivity measurement

Conductivity measurements were carried out by a four-point probe method. The blends of PANI

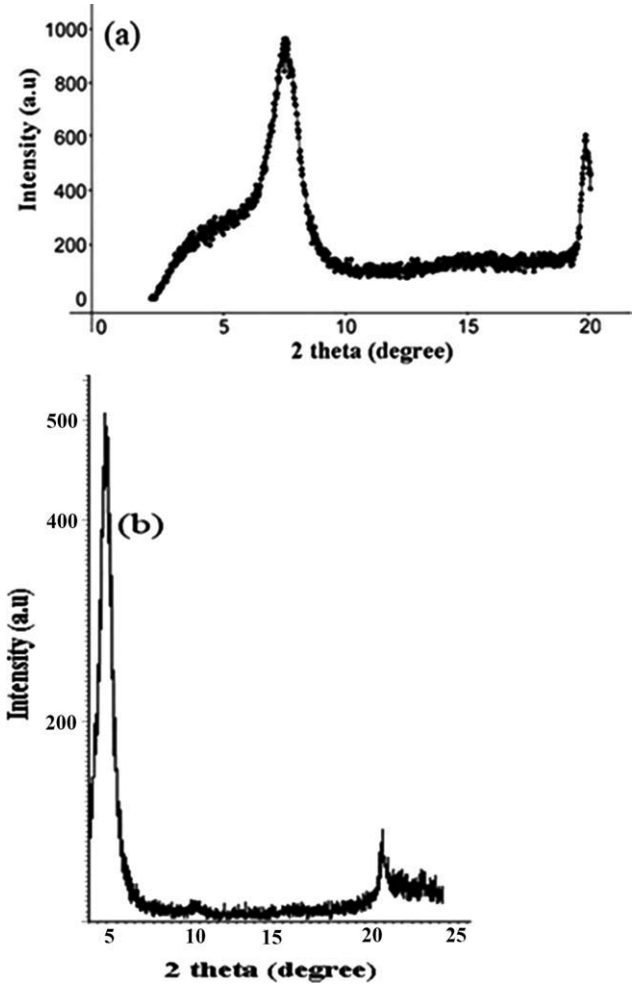

Figure 6 XRD patterns of the (a) parent MMT and (b) organomodified MMT.

nanocomposites were compacted into pellets for measurements. The reported conductivity values were the averages of four pairs of readings at different parts on both sides of the pellets. All measurements were done in air at room temperature and converted to conductivity by the following equation:

$$\rho = 1/\delta = V/I\omega\pi/\ln 2$$

where ρ is the resistivity (Ω cm), δ is the conductivity (s/cm), V is the potential difference (mV), I is the applied constant current (mA), and ω is the thickness (cm).

The conductivity of the nanocomposite was low compared to that of PANI. The main reason seemed to be stereochemical differences between these two conducting polymers. Oxidized PANI had an almost planar structure with a low ionization potential due to strong delocalization of the electrons. The conductivity values of the pure PANI and terpolymer [(PSt-*co*-PMSt)-*g*-PANI] were 1.25 and 0.17 S cm^{-1}, respectively.

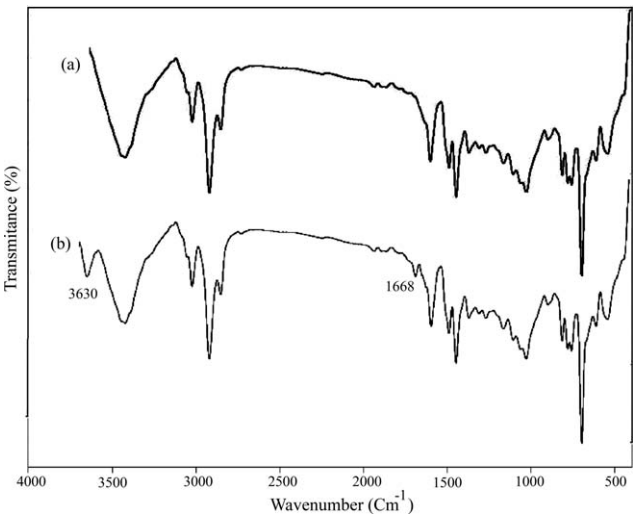

Figure 7 FTIR spectra of (a) PANI and (b) (PSt-*co*-PMSt)-*g*-PANI/OMMT nanocomposite.

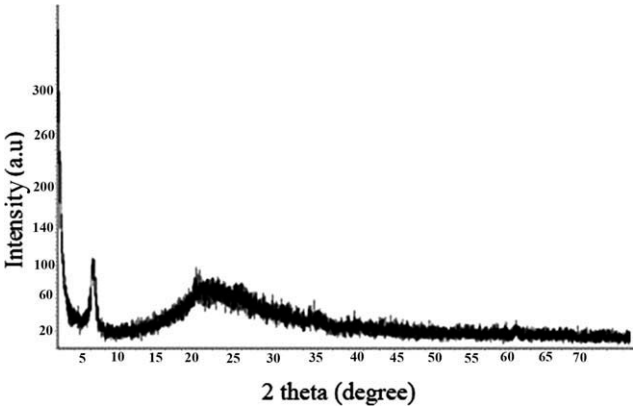

Figure 8 XRD patterns of (PSt-*co*-PMSt)-*g*-PANI/OMMT nanocomposite.

Figure 5(a,b) shows the FTIR spectra of the unmodified MMT and modified MMT. In the spectra of both the modified and unmodified clays, the intense band at 1045 cm^{-1} and the two bands at 467 and 525 cm^{-1} were assigned to Si—O band stretching and Si—O band bending, respectively. Unreacted hexadecyl trimethyl ammonium chloride showed characteristic bands at 1637 cm^{-1}, which was attributed to ammonium groups. The band around 3630 cm^{-1} was due to the stretching of —Si—OH groups in the clay. The FTIR spectra of the modified clay exhibited an absorption band at 1467 cm^{-1}, attributed to C—H bending bands. In addition, the intercalation of the modifier instead of sodium ions was confirmed by the C—H stretching vibration at 2855 and 2925 cm^{-1}.

Figure 6(a,b) shows the XRD patterns of the parent MMT and the organomodified MMT. An increase of the basal spacing (d_{001}) of the modified clay was observed after the insertion of the surfactant. More specifically, the pristine MMT showed a

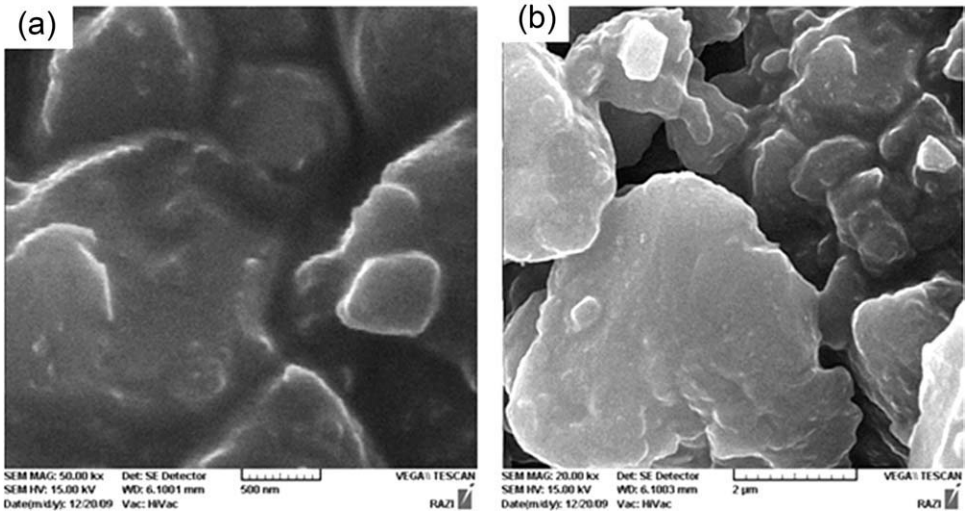

Figure 9 SEM images for the (PSt-*co*-PMSt)-*g*-PANI/OMMT nanocomposite.

d_{001}-spacing of 12.6 Å; this corresponded to an interlayer spacing (D) of 12.6 − 9.6 = 3 Å, where 9.6 Å is the thickness of the individual clay sheet. In the case of the organoclay, the basal spacing (d_{001}) became 18.38 Å with a corresponding interlayer spacing of D = 8.66 Å.

Characterization of the nanocomposites

Figure 7 shows the FTIR spectra of the PANI [Fig. 7(a)] and (PSt-*co*-PMSt)-*g*-PANI/OMMT nanocomposite [Fig. 7(b)]. Apparently, the FTIR spectrum of the nanocomposite showed a combination of organomodified MMT and terpolymer. The band around 3630 cm^{-1} was due to the stretching of —Si—OH groups in the clay. Other additional bands observed in the spectrum of the (PSt-*co*-PMSt)-*g*-PANI/OMMT nanocomposite arose from terpolymer stretching or bending bands. FTIR spectrum assignments verified that the OMMT layers were doped into the polymer matrix during the solution intercalation and, thus, formed the (PSt-*co*-PMSt)-*g*-PANI/OMMT nanocomposite.

XRD provided information on the changes of the interlayer spacing of the clay upon the formation of the nanocomposite. The formation of an intercalated structure should result in a decrease in 2θ, which indicates an increase in the *d*-spacing; the formation of an exfoliated structure usually results in the complete loss of registry between the clay layers, and no peak was seen in the XRD trace. In some cases, a disordered immiscible system was obtained, and this also showed no peaks, so the absence of an XRD peak could not be taken as definitive evidence for the formation of a exfoliated nanocomposite, and additional evidence, usually transmission electron microscopy or scanning electron microscopy (SEM)

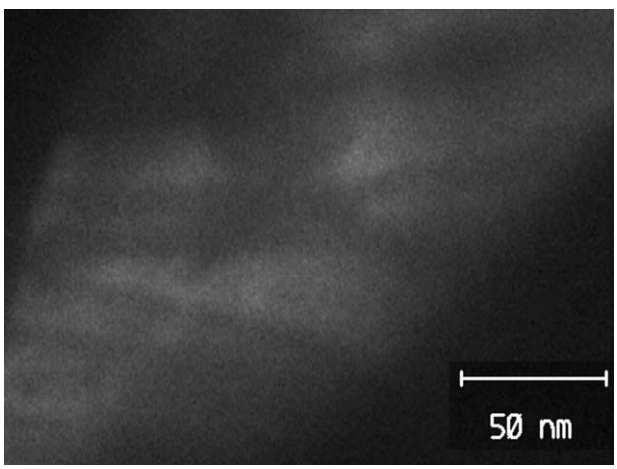

Figure 10 Transmission electron microscopy images for the (PSt-*co*-PMSt)-*g*-PANI/OMMT nanocomposite.

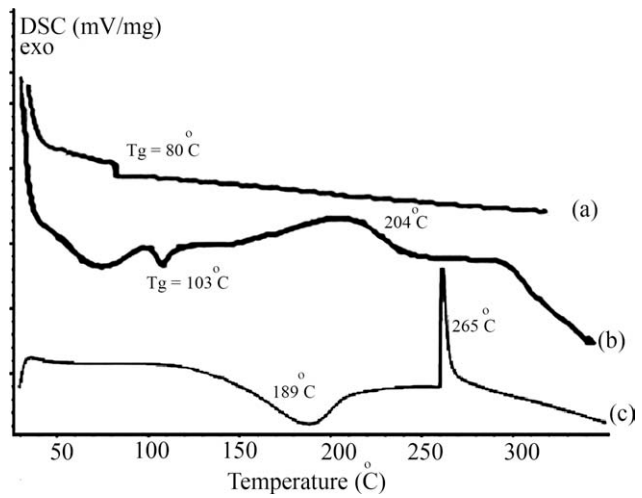

Figure 11 DSC traces of (a) PSt-*co*-PMSt, (b) neat (PSt-*co*-PMSt)-*g*-PANI, and (c) (PSt-*co*-PMSt)-*g*-PANI/OMMT nanocomposite.

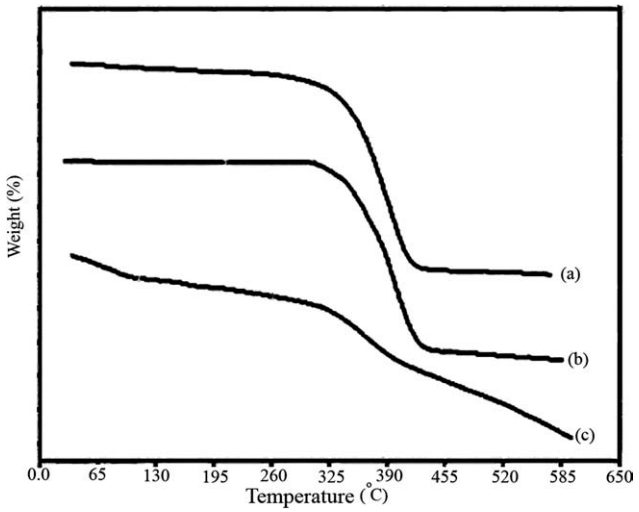

Figure 12 TGA thermograms of (a) PSt-*co*-PMSt, (b) (PSt-*co*-PMSt)-*g*-PANI, and (c) (PSt-*co*-PMSt)-*g*-PANI/OMMT nanocomposite.

analysis, is required. Figure 8 presents the XRD data for the (PSt-*co*-PMSt)-*g*-PANI/OMMT nanocomposite. The broad peak with 2θ around 22.7° and the peak with 2θ around 6.1° were related to the diffraction of amorphous PANI. For the nanocomposite, no peaks were observed related to the organophilic clay nanocomposite; this could have meant that either an exfoliated or an immiscible nanocomposite was formed.

SEM characterization of the nanocomposites

SEM provides an actual image of the morphology of the nanocomposite. SEM is complementary to XRD, especially when peaks are not observed in XRD. Figure 9 shows the SEM images for the (PSt-*co*-PMSt)-*g*-PANI/OMMT nanocomposite, which indicated that clay was well dispersed in the polymeric matrix and showed the formation of an exfoliated nanocomposite.

Figure 10 reveals that the nanocomposites were in a much exfoliated state. The dark lines indicate the MMT layers with a thickness of about 1 nm. In Figure 10, nanosized MMT aggregates could be detected in various degrees; this might have been due to intercalated or partially exfoliated structures. This observation was consistent with the XRD results. If the silicates were dispersed randomly and homogeneously in the polymer matrix, the interface area would have been enormous, and pronounced interaction could be expected.

Glass transition of the (PSt-*co*-PMSt)-*g*-PANI/OMMT nanocomposites

Figure 11(a–c) shows the DSC thermogram of the PSt-*co*-PMSt, neat terpolymer, and (PSt-*co*-PMSt)-*g*-PANI/OMMT nanocomposites, respectively. PSt-*co*-PMSt exhibited an endothermic peak at approximately 80°C; this corresponded to the glass-transition temperature (T_g). The endothermic peaks seen at 81°C in Figure 11(b) were attributed to the evaporation of any residual water and solvent. A strong endothermic peak seen at 103°C, corresponding to T_g, and an exothermic peak at 204°C indicated the degradation of this copolymer. Figure 11(c) exhibits an exothermic peak at 265°C corresponding to the degradation of the copolymer. The transition appearing at 189°C could be attributed to the glass transition of this sample. PSt chains bonded to the backbone of PANI led to more flexibility in the copolymer structure and caused degradation at lower temperatures. The thermogram also confirmed the absence of any melting for all of the samples.

Thermal stability of the (PSt-*co*-PMSt)-*g*-PANI/OMMT nanocomposites

The characteristic TGA curves of the PSt-*co*-PMSt, terpolymer, and (PSt-*co*-PMSt)-*g*-PANI/OMMT nanocomposite are shown in Figure 12. The TGA results indicate an improvement in the thermal stability for the terpolymer compared to that of the PSt-*co*-PMSt copolymer and a higher thermal stability for the (PSt-*co*-PMSt)-*g*-PANI/OMMT nanocomposite (3 wt % OMMT) compared to that of the neat terpolymer.

The thermal stability and the combustion behavior of the polymer–clay nanocomposite was affected by the degradation mechanism of the surfactant molecules. During the thermal treatment of the nanocomposite at elevated temperatures, acidic proton sites were formed via the Hoffman decomposition of the alkyl ammonium modifier of the clay; this gave a protonated MMT that could act as a protonic acid catalyst. Camino et al.[32] ascribed the lower thermal stability of an epoxy resin composite, when compared to those of the other filled composites, to the larger catalytic activity related to the monoalkyl structure of its organic modifier compared to the dialkyl to tetraalkyl substitution of the other clays.

CONCLUSIONS

The reaction of PANI in the emeraldine state with (PSt-*co*-PMSt)-Br was investigated in this work. PSt-*co*-PMSt was prepared by an NMRP method. Then, NBS was used as a brominating agent to obtain copolymers with bromine. The solution terpolymer derived from styrene, methyl styrene, and PANI was synthesized through an *N*-grafting reaction of deprotonated PANI by BuLi and a brominated terpolymer. Then, the exfoliated PANI-grafted poly(St-*co*-MSt) copolymer/organomodified MMT [(PSt-*co*-PMSt)-*g*-PANI/OMMT] nanocomposites were synthesized by

a solution intercalation method. The investigation of the thermal behavior of the terpolymers showed the increased flexibility compared to that of PANI and a higher thermal stability compared to that of PSt-*co*-PMSt because of the substitution. The thermal stability and T_g of the nanocomposite improved observably in comparison with those of the pure terpolymer.

The author expresses their gratitude to the "Iran National Science Foundation" (INSF) and Tabriz Payame Noor University for supporting of this project.

References

1. Chinn, D.; DuBow, J.; Liess, M.; Josowicz, M.; Janata, J Chem Mater 1995, 7, 1504.
2. Tsutsumi, H.; Yamashita, S.; Oishi, T. J Appl Electrochem 1997, 27, 477.
3. Paul, E. W.; Rico, A. J.; Wrighton, M. S. J Phys Chem 1985, 89, 1441.
4. Lee, Y. H.; Kim, C. A.; Jang, W. H.; Choi, H. J.; Jhon, M. S. Polymer 2001, 42, 8277.
5. Sangodkar, H.; Sukeerthi, S.; Srinivasa, R. S.; Lal, R.; Contractor, A. Q. Anal Chem 1996, 68, 779.
6. Bossi, A.; Piletsky, S. A.; Piletska, E. V.; Righetti, P. G.; Turner, A. P. F. Anal Chem 2000, 72, 4296.
7. Mu, S. Macromol Chem Phys 2005, 206, 689.
8. Kulkarni, M.; Viswanath, A. K. Eur Polym J 2004, 40, 379.
9. Chen, Y.; Kang, E. T.; Neoh, K. G.; Ma, Z. H.; Tan, K. L. Macromol Chem Phys 2001, 202, 785.
10. Hosseini, S. H. J Appl Polym Sci 2006, 101, 3920.
11. Lee, X.; Guo, X.; Zhang, L.; Wang, Y.; Su, Z. J Appl Polym Sci 2007, 103, 140.
12. Lee, C. W.; Seo, Y. H.; Lee, S. H. Macromolecules 2004, 37, 4070.
13. Zheng, W. Y.; Levon, K.; Laakso, J.; Osterholm, J. E. Macromolecules 1994, 27, 7754.
14. Wang, P.; Tan, K. L.; Zhang, F.; Kang, E. T.; Neoh, K. G. Chem Mater 2001, 13, 581.
15. Arsalani, N.; Khavei, M.; Entezami, A. A. Iran Polym J 2003, 12, 237.
16. Yu, Y. J.; Che, B.; Si, Z. H.; Li, L.; Chen, W.; Xue, G. Synth Met 2005, 150, 271.
17. Long, Y. Z.; Chen, Z. J.; Duvail, J. L.; Zhang, Z. M.; Wan, M. X. Physica B 2005, 370, 121.
18. Ray, S. S.; Biswas, M. Synth Met 2000, 108, 231.
19. Zhang, L. J.; Wan, M. X.; Wei, Y. Synth Met 2005, 151, 1.
20. Wu, Q. Z.; Xue, Z.; Qi, Z.; Wang, F. Polymer 2000, 41, 2029.
21. Cao, Y.; Li, S.; Xue, Z.; Guo, D. Synth Met 1986, 16, 305.
22. Govindara, N.; Mortland, M. M.; Boyd, S. A. Environ Sci Technol 1987, 21, 1119.
23. Bani, F.; Abbasian, M.; Afshar Taromi, F.; Entezami, A. Iran Polym J 2004, 13, 513.
24. Abbasian, M.; Namazi, H.; Entezami, A. Polym Adv Technol 2004, 15, 606.
25. Mohajeri, S.; Najafi Moghaddam, P.; Rahmani, S.; Entezami, A. Polym Adv Technol 2010, 21, 65.
26. Abbasian, M.; Entezami, A. A. Polym Adv Technol 2007, 18, 306.
27. Kaplan, S.; Conwell, E. M.; Richter, A. F.; MacDiarmid, A. G. Macromolecules 1989, 22, 1669.
28. Moad, G.; Rizzardo Thang, S. H.; Aus J Chem 2005, 58, 379.
29. Salaneck, W. R.; Liedberg, B.; Ingana, S. O.; Erlandsson, R.; Lundstörm, I.; MacDiarmid, A. G.; Halpern, M.; Somasiri, N. L. D. Mol Cryst Liq Cryst 1985, 121, 191.
30. Zhao, B.; Neoh, K. G.; Kang, E. T.; Tan, K. L. Chem Mater 2000, 12, 1800.
31. Tarkuc, S.; Sahin, E.; Toppare, L.; Colak, D.; Cianga, I.; Yagci, Y. Polymer 2006, 47, 2001.
32. Camino, G.; Tartaglione, G.; Frache, A.; Manferti, C.; Costa, G. Polym Degrad Stab 2005, 90, 354.